Rapid Self-Healing and Thixotropic Organogelation of Amphiphilic Oleanolic Acid–Spermine Conjugates

*Zulal Özdemir,[a,b] David Šaman,[c,‡] Kia Bertula,[d,‡] Manu Lahtinen,[e,‡] Lucie Bednárová,[c,‡] Markéta Pazderková,[c,f,‡] Lucie Rárová,[g] Nonappa *[,d,h] and Zdeněk Wimmer *[,a,b]*

[a] University of Chemistry and Technology in Prague, Department of Chemistry of Natural Compounds, Technická 5, 16028 Prague 6, Czech Republic. E-mail: zdenek.wimmer@vscht.cz

[b] Institute of Experimental Botany of the Czech Academy of Sciences, Isotope Laboratory, Vídeňská 1083, 14220, Prague 4, Czech Republic. E-mail: wimmer@biomed.cas.cz

[c] Institute of Organic Chemistry and Biochemistry of the Czech Academy of Sciences, Flemingovo náměstí 2, 16610 Prague 6, Czech Republic

[d] Aalto University, Department of Applied Physics, Puumiehenkuja 2, FI-02150 Espoo, Finland. Email: nonappa@aalto.fi

[e] University of Jyväskylä, Department of Chemistry, P. O. Box. 35, FI-40014 Jyväskylä, Finland

[f] Charles University, Institute of Physics, Faculty of Mathematics and Physics, Ke Karlovu 5, 12116 Prague 2, Czech Republic

[g] Laboratory of Growth Regulators, Institute of Experimental Botany of the Czech Academy of Sciences, and Faculty of Science, Palacký University, Šlechtitelů 27, CZ-78371 Olomouc, Czech Republic

[h] Tampere University, Faculty of Engineering and Natural Sciences, P.O. Box 541, FI-33101 Tampere, Finland. Email: nonappa.nonappa@tuni.fi

KEYWORDS. Oleanolic acid; spermine; amphiphile; thixotropy; self-healing; supramolecular gel; rheology.

ABSTRACT. Natural and abundant plant triterpenoids are attractive starting materials for the synthesis of conformationally rigid and chiral building blocks for functional soft materials. Here we report the rational design of three oleanolic acid-triazole-spermine conjugates, containing either one or two spermine units in the target molecules, using Cu(I)-catalyzed Huisgen 1,3-dipolar cycloaddition reaction. The resulting amphiphile-like molecules **2** and **3**, bearing just one spermine unit in the respective molecules, self-assemble into highly entangled fibrous network leading to gelation at a concentration as low as 0.5 % in alcoholic solvents. Using step-strain rheological measurements, we show rapid self-recovery (up to 96 % of initial storage modulus) and sol ⇔ gel transition under several cycles. Interestingly, rheological flow curves reveal thixotropic behavior of the gels. To the best of our knowledge this kind of behavior was not shown in the literature before, neither for a triterpenoid nor for its derivatives. The conjugate **4**, having bolaamphiphile-like structure, was found to be a non-gelator. Our results indicate that the position and number of spermine units alter the gelation properties, gel strength, and their self-assembly behavior. Preliminary cytotoxicity studies of the target compounds **2**–**4** in four human cancer cell lines suggest that the position and number of spermine units affects the biological activity. Our results also encourage exploring other triterpenoids and their derivatives as sustainable, renewable and biologically active building blocks for multifunctional soft organic nanomaterials.

Introduction

Supramolecular gels resulting from the self-assembly of low molecular mass organic compounds represent an important class of soft materials having their potential in applications in functional materials, catalysis, optoelectronics and sensors.[1-5] Low molecular weight gelators (LMWGs), undergo hierarchical assembly into highly entangled fibrous networks capable of immobilizing a large number of solvent molecules.[6] Despite being predominantly comprised of liquids, the resulting gels display solid-like mechanical properties in their rheological behavior.[7] Importantly, in general molecular organo- and hydrogels offer reversible control of their mechanical properties when perturbed by external stimuli, such as temperature,[7] light,[8] electric field,[9] pH,[10] oxidation-reduction,[11] or mechanical stress.[12] The reversible mechanical properties are consequences of the structural reorganization of gelators.[4] The microscopic changes occurring in molecular gels are attributed to non-covalent intermolecular interactions responsible for the molecular self-assembly. The non-covalent interactions such as hydrogen bonding,[13] electrostatic effect,[14] hydrophobic effect,[15] London dispersion forces,[16] van der Waals interactions,[17] charge-transfer complexation,[18] metal coordination,[19-21] halogen bonding,[22] and fluorine-fluorine interactions[23,24] have been explored effectively for designing new gelators. Extensive research, pursued over the last three decades on diverse building blocks, has offered the possibilities towards the rational design of molecular gelators with unique material properties. The building blocks ranging from long chain hydrocarbons,[15] peptides,[25] polyaromatics,[18] steroids,[26-32] carbohydrates,[33] and metal complexes,[19-21] have been studied extensively. Molecular gels are generally considered as kinetically trapped metastable state, and the gelation process can be controlled by tuning the supramolecular interactions and self-assembly pathways to obtain different material properties.[34,35] It has been shown that there is a

delicate balance between gelation and crystallization. Therefore, gelation is often considered as failed crystallization.[36,37] It has been shown that this balance between gel state and the crystallization depends on the activation barrier.[38]

Molecular gels with a wide range of morphologies including tapes, ribbons, fibers and microcrystalline networks have been reported in the literature.[1-5] More importantly, self-assembly of chiral gelator molecules has also been shown to exhibit amplification of chirality upon gelation,[14,39-42] and in some cases formation of helical fibers, twisted tapes or ribbons have been visualized using electron microscopy (EM).[43,44] Molecular gels also display self-healing and thixotropic behavior making them attractive for industrial, pharmaceutical and cosmetic applications.[45-46] Self-healing gels recover their initial properties , e.g., modulus or shape, after subjecting for physical, chemical or mechanical perturbations.[47-49] Self-healing properties of molecular gels can be determined using visual demonstration, oscillatory rheology and cyclic compression/tensile testing.[50] While visual demonstration is a qualitative method, step-strain rheological experiments allow quantitative determination of structure recovery. Importantly, step-strain experiments are suitable for low molecular gels even with very low solid content.

On the other hand, thixotropic gels undergo a transition from gel to solution upon applying stress. However, they recover back to the original gel state when there is no applied shear.[51,52] According to the IUPAC definition, thixotropy is defined as *"the continuous decrease of viscosity with time when flow is applied to a sample that has been previously at rest, and the subsequent recovery of viscosity when flow is discontinued"*.[53] Unlike shear thinning behavior, i.e., decrease in viscosity upon increasing shear stress, thixotropy is a time dependent property. Thixotropic behavior can be studied by time dependent step-strain and rate dependent shear stress *versus* shear rate oscillatory rheological experiments.[47] Recovery of the gel is observed

after shearing in rate dependent shear stress *versus* shear rate experiment. However, when the gel recovers back to its original modulus, it does not follow the exact path, instead it shows a hysteresis loop, indicating the thixotropic behavior of the gels. The thixotropic properties are generally exhibited by molecular gels composed of the non-crystalline network.[54-56] However, there is no specific design strategy available to prepare such gels.[57]

Irrespective of the nature of the gels and the diversity of building blocks, amphiphilicity has been a common property in a large number of LMWGs.[5] Furthermore, a certain class of gelators such as cholesterol,[27] bile acids,[26] plant sterols,[58-62] and sorbitol displays varying degree of conformational rigidity, which facilitates a reduction in the entropic losses upon self-assembly.[63,64] Contrary to other gelators, strong hydrogen bonding interactions are absent in several conformationally rigid gelators, and even if they are present, they contribute to a lesser extent towards self-assembly.[5] However, in the field of soft materials, plant triterpenoids are a much less explored class of conformationally rigid, naturally abundant, renewable and sustainable resources.[65] Triterpenoids, being structurally different from steroids, are a class of triterpenes, compounds with 30 carbon atoms, either in linear structure or fused rings, but containing additional heteroatoms or functional groups.[66] They are precursors for steroids, which compounds, contrary to triterpenoids, are characterized by at least 17 carbon atoms and bear tetracyclic systems with three six-membered rings (A, B and C) and a five-membered ring (D).[67] This class of compounds, including cholesterol (a sterol), and bile acids, has already been extensively studied for their self-assembly and gelation properties.[1-5,10,26-32]

Oleanolic acid [(3β)-3-hydroxyolean-12-en-28-oic acid, **1**] is a pentacyclic triterpenoid (Figure 1) found throughout the plant kingdom in more than 120 plant species, of which especially in *Panax ginseng* root and *Sambucus chinensis* (Chinese elder) in high concentrations.[68,69] It

displays a wide range of modest biological activities, including antitumor effects.[70-73] Studies on the self-assembly of triterpenoids have been limited to betulinic acid, arjunolic acid, ursolic acid, glycyrrhetinic acid, and oleanolic acid in a few selected organic solvents.[74-76] At relatively high concentrations, gelation of oleanolic acid has also been reported in organic solvents.[74,75] Oleanolic acid is a lipophilic compound displaying low bioavailability,[68] and the functional group chemistry of oleanolic acid has not yet been fully exploited for the synthesis of its derivatives. Therefore, it is desirable to address whether naturally abundant oleanolic acid can be functionalized to obtain amphiphilic building blocks. Such a design requires a careful and selective chemical transformation. Towards this end, naturally occurring sterol-spermine conjugates, such as squalamine, has inspired the synthesis of spermine conjugates of fatty acids and steroids as polycationic amphiphiles.[77,78] The spermine conjugates have been shown to efficiently bind to DNA, and act as non-viral gene carriers and ionophores.[79-84] The synthetic spermine conjugates have been shown to exhibit a broad spectrum of antimicrobial activities,[85-87] and reported to self-assemble into molecular gels.[88,89] Previously, the synthesis of different triterpenoid-polyamine conjugates *via* the amide bond formation has been studied and the compounds were subjected to the selected pharmacological screening tests.[90-92]

Herein, we aimed to explore the possibilities to design oleanolic acid-triazole-spermine conjugates as polycationic amphiphiles, to study their self-assembly behavior, potential gelation, morphological features and mechanical properties. To achieve this objective, we have undertaken the following tasks. (a) The Cu(I)-catalyzed Huisgen 1,3-dipolar cycloaddition reaction has been used as one of the key steps to prepare oleanolic acid-triazole-spermine conjugates (Figure 1). Accordingly, three derivatives were prepared by appending spermine conjugates at C(3)-OH (**2**), C(17)-COOH (**3**), and both C(3)-OH and C(17)-COOH (**4**) by

selective chemical transformations (Scheme 1). (b) We show that the synthesized conjugates **2** and **3** act as LMWGs when tested in alcoholic solvents, resulting in highly entangled fibrous networks. The VC and VT NMR spectroscopy, IR spectroscopy, X-ray powder diffraction techniques, thermal analysis and electron microscopy were used to investigate supramolecular self-assembly of the target compounds. (c) Using extensive oscillatory rheological measurements and using a visual demonstration, we have shown that the gels exhibit rapid self-healing and thixotropic behavior. (d) Finally, the target compounds **2**–**4** were subjected to a cytotoxicity screening tests in four cancer cell lines, exhibiting differences in cytotoxicity values that depended on the structure of conjugates.

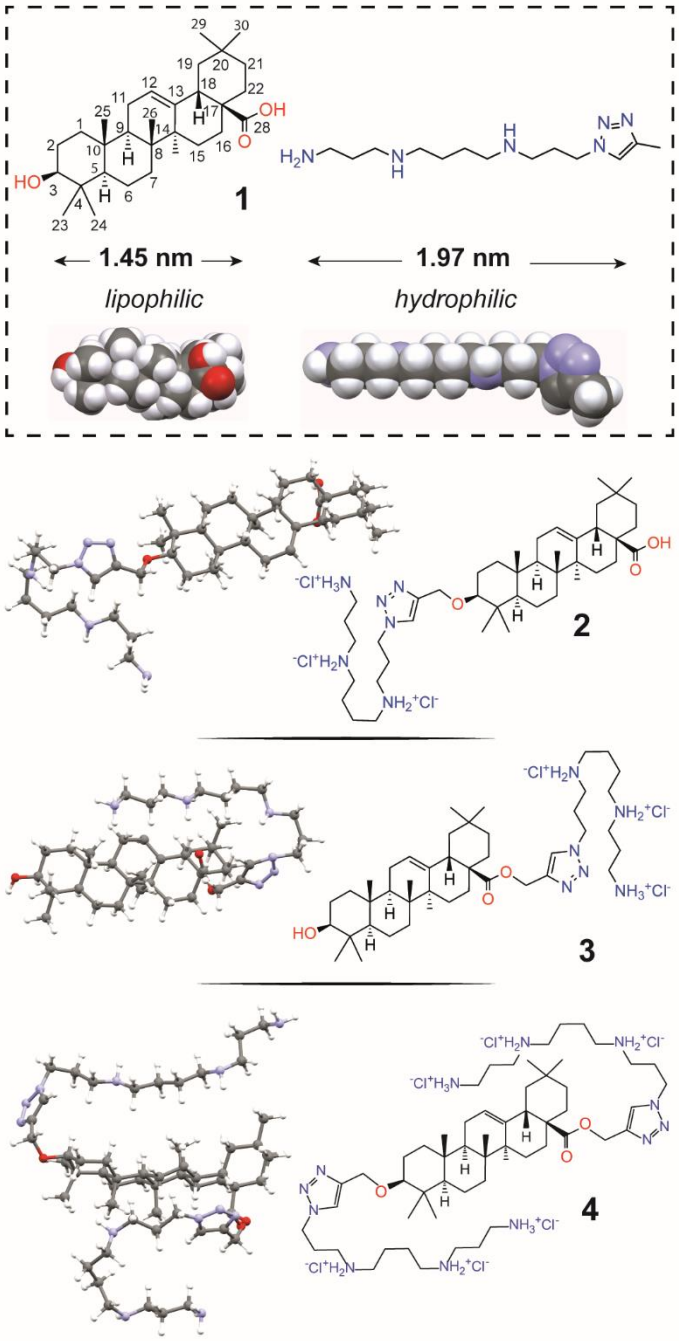

Figure 1. Chemical structures of the target compounds studied in this work. Oleanolic acid (**1**) and its space filling model based on the X-ray single crystal structure (*CSD entry: VUZVUI*; top left), space filling model of the triazole-spermine conjugate based on its energy minimized

structure (top right), and oleanolic acid-triazole-spermine conjugates **2**–**4** along with their energy minimized structures.

Scheme 1. Synthesis of oleanolic acid-triazole-spermine conjugates **2**–**4**.

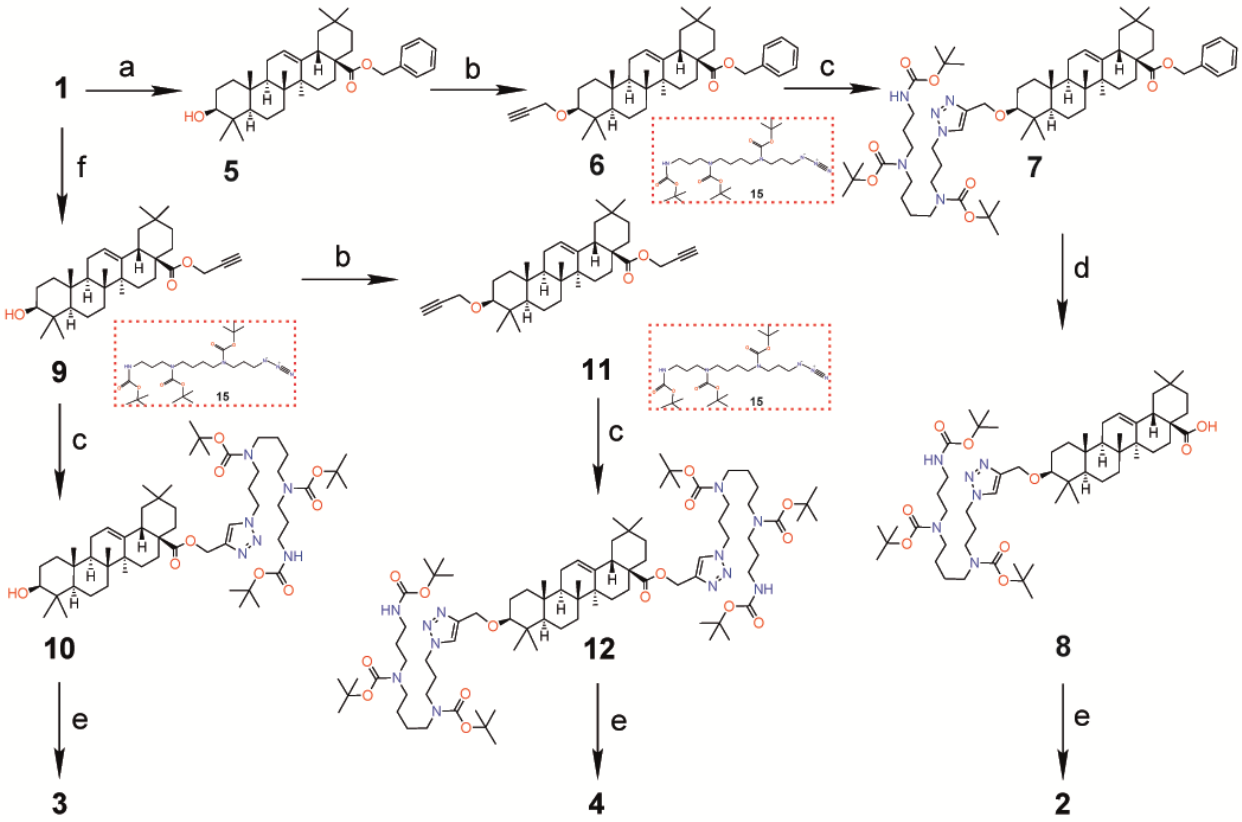

a) Benzyl bromide, K_2CO_3, in DMF, rt; b) propargyl bromide, NaH (60 % dispersion in mineral oil), in THF, rt; c) **15**, $CuSO_4 \cdot 5H_2O$/TBTA, sodium ascorbate, in DCM/H_2O, rt; d) Pd/C (10 %), H_2, in THF/EtOH rt; e) 1.0 M HCl, in ethyl acetate, rt; f) propargyl bromide, K_2CO_3, in DMF, rt.

Experimental section

General

The ^{1}H and ^{13}C nuclear magnetic resonance (NMR) spectra were recorded on a Bruker AVANCE 600 MHz spectrometer at 600.13 MHz and 150.90 MHz in $CDCl_3$ or CD_3OD, using tetramethylsilane ($\delta = 0.0$) as internal reference. ^{1}H NMR spectral data are presented in the following order: chemical shift (δ) expressed in ppm, multiplicity (s, singlet; d, doublet; t, triplet; q, quartet; m, multiplet), coupling constants in Hertz, number of protons. For unambiguous assignment of both ^{1}H and ^{13}C signals 2D NMR ^{1}H,^{13}C gHSQC and gHMBC spectra were measured using standard parameters sets and pulse programs delivered by producer of the spectrometer. Infrared spectra (IR) were measured with Nicolet 6700 FT-IR spectrometer (USA) equipped with standard mid-IR source, KBr beam-splitter, DTGS detector and with the cell compartment purged by dry nitrogen during all the measurements. Mass spectra (MS) were measured with a Waters ZMD mass spectrometer in a positive or negative electrospray ionization mode. Optical rotations were measured on an Autopol IV instrument (Rudolph Research Analytical, USA) at 589 nm wavelength, and the values were corrected to 20 ºC. All other instruments used in a detailed investigation of supramolecular systems (scanning electron microscopy, transmission electron microscopy, rheometer, X-Ray diffractometer, thermogravimetric analyzer) are described in the Supporting Information. Thin layer chromatography (TLC) was carried out on silica gel plates (Merck $60F_{254}$) and the visualization was performed using UV detection and by spraying with the methanolic solution of phosphomolybdic acid (5 %) followed by heating. For column chromatography, silica gel 60 (0.063-0.200 mm) from Merck was used. All chemicals and solvents were purchased from regular commercial sources in analytical grade and the solvents were purified by general

methods before use. Oleanolic acid was purchased from Dr. Jan Šarek – Betulinines (www.betulinines.com).

Procedure for preparation of compound **2**

Synthesis of compound **5**

Benzyl bromide (235 µL, 1.97 mmol) and K_2CO_3 (272 mg, 1.97 mmol) were added to a solution of **1** (600 mg, 1.31 mmol) in DMF (10 mL) in a round bottom flask. The mixture was stirred at r. t. for 17 h. The reaction was monitored using TLC and upon complete conversion of the starting materials to product, the reaction was quenched by adding water to the reaction medium. The reaction mixture was extracted into benzene and washed with brine solution (5 × 50 mL) using a separatory funnel. The organic layer was dried over anhydrous Na_2SO_4, filtered, and removed under reduced vacuum to obtain the crude product. The crude product was column purified on silica gel using 50/50 v/v (%) petroleum ether/chloroform to 100 % chloroform to afford **5** in a 94 % yield as a white solid.

Synthesis of compound **6**

Sodium hydride (60 % dispersion in mineral oil; 1049 mg, 26.24 mmol) was added to a solution of **5** (896 mg, 1.64 mmol) in dry THF (15 mL) as two portions within 2 h intervals in a round bottom flask. The mixture was stirred at r. t. for 4 h. When the color of the solution turned creamy grey, propargyl bromide (425 µL, 4.91 mmol) was added to reaction mixture drop by drop under the argon atmosphere. After stirring at r. t. for 5 days, excess sodium hydride was neutralized by slow addition of water. The reaction mixture was extracted to chloroform using a

separatory funnel and dried over anhydrous Na_2SO_4. The volatiles were removed under reduced pressure. The crude product obtained after aqueous work up was column purified on silica gel using 50/50 v/v (%) petroleum ether/chloroform to 100 % chloroform to afford **6** in a 76 % yield as a white-yellowish solid.

Synthesis of compound **7**

Compound **15** (529 mg, 1.0 mmol) was added to a stirred solution of **6** (450 mg, 0.77 mmol) in DCM (7 mL) in a round bottom flask, followed by $CuSO_4 \cdot 5H_2O$/TBTA (1:1) complex solution (7.7 mL, 0.39 mmol) and stirred at r. t. for 5 min. To the above mixture, sodium ascorbate (152 mg, 0.77 mmol) was added, and the contents were mixed at r. t. for 20 h. The reaction mixture was then extracted by $CHCl_3$ and washed with water. After drying the organic layer over anhydrous Na_2SO_4, the volatiles were removed under reduced pressure. The crude product obtained after aqueous work up was column purified on silica gel using ethanol in chloroform [from 100/0 v/v (%) to 100/5 v/v (%)] to afford **7** in a 99 % yield as a white foam.

Synthesis of compound **8**

Catalyst (Pd/C (10 %); 550 mg, 0.52 mmol) was added to a solution of **7** (860 mg, 0.77 mmol) in a THF/ethanol mixture (10/10 mL). The reaction vessel was repeatedly degassed under vacuum and flushed with argon four times. The catalytic hydrogenation was carried out under a hydrogen atmosphere at r. t. for 27 h. The reaction mixture was filtered using a sintered glass funnel to remove solid. The filtrate was collected and evaporated under reduced pressure to furnish white solid that was purified by column chromatography using a gradient mobile phase ethanol/chloroform [from 100/0 v/v (%) to 100/2 v/v (%)] to afford **8** in a 90 % yield as a white foam.

Synthesis of compound **2**

A solution of HCl (gas; 1.0 M in ethyl acetate; 48 mL, 47.41 mmol) was added to a solution of **8** (0.63 mmol, 1 eq.) and the reaction mixture was stirred at r. t. for 24 h. The resulting white residue was filtered and washed with ethyl acetate to furnish **2** as a white solid in a 95 % yield.

Procedure for preparation of compound **3**

Synthesis of compound **9**

Propargyl bromide (115 μL, 1.31 mmol) and K_2CO_3 (182 mg, 1.31 mmol) were added to a solution of **1** (400 mg, 0.88 mmol) in DMF (5 mL). The reaction mixture was stirred at r. t. for 48 h. The reaction was monitored using TLC and quenched by the addition of water to the reaction medium. The mixture was extracted using benzene and washed brine solution (5 × 50 mL). The organic layer was dried over by Na_2SO_4, filtered and evaporated under vacuum. The crude product obtained after aqueous work up was column purified on silica gel using chloroform to afford **9** in a 98 % yield as a white solid.

Synthesis of compound **10**

Compound **15** (340 mg, 0.64 mmol) was added to a stirred solution of **9** (266 mg, 0.54 mmol) in DCM (5.4 mL), followed by $CuSO_4 \cdot 5H_2O$/TBTA (1:1) complex solution (0.27 mmol, 5.4 mL) and stirred at r. t. After stirring for five min, sodium ascorbate (106 mg, 0.54 mmol) was added to the mixture, and the content was mixed at r. t. for 27 h. It was extracted into $CHCl_3$ and washed with H_2O. After drying the organic layer over anhydrous Na_2SO_4, the volatiles were

removed under reduced pressure. The crude product obtained after aqueous work up was column purified on silica gel using ethanol in chloroform [from 100/0 v/v (%) to 100/4 v/v (%)] affording **10** as a white foamy solid in a 99 % yield.

Synthesis of compound **3**

A solution of HCl (gas; 1.0 M in ethyl acetate; 31 mL, 31.30 mmol) was added to a solution of **8** (433 mg, 0.42 mmol) and the reaction mixture was stirred at r. t. for 18 h. The resulted white residue was filtered using a sintered glass funnel, washed with diethyl ether, and white crystals were obtained with a 97 % yield.

Procedure for preparation of compound **4**

Synthesis of compound **11**

Sodium hydride (60 % dispersion in mineral oil; 129 mg, 3.23 mmol) was added to a solution of **9** (100 mg, 0.20 mmol) in dry THF in two portions within 2 h intervals. The reaction mixture was stirred at r. t. for 4 h. When the color of solution turned creamy grey, propargyl bromide (70 µL, 0.80 mmol) was added to the reaction mixture drop by drop under the argon atmosphere. After stirring at r. t. for four days, excess of sodium hydride was neutralized by a slow addition of water. The mixture was extracted into an organic layer using chloroform. After drying the organic layer over anhydrous Na_2SO_4, the volatiles were removed under reduced pressure. The crude product obtained after aqueous work up was column purified on silica gel using petroleum ether in chloroform [from 50/50 v/v (%) to 0/100 v/v (%)] to afford **11** in a 91 % yield as a pale yellowish solid.

Synthesis of compound **12**

Compound **15** (338 mg, 0.64 mmol) was added to a stirred solution of **11** (142 mg, 0.27 mmol) in DCM, followed by a $CuSO_4 \cdot 5H_2O$/TBTA (1:1) complex solution (5.33 mL, 0.27 mmol). After stirring the reaction mixture for five min, sodium ascorbate (105 mg, 0.53 mmol) was added to the mixture and stirred at r. t. for 24 h. It was then extracted into $CHCl_3$ and washed with brine. After drying the organic layer over anhydrous Na_2SO_4, the volatiles were removed under reduced pressure. The crude product obtained after aqueous work up was column purified on silica gel using ethanol in chloroform [from 100/1.5 v/v (%) to 100/4.5 v/v (%)] afford **12** in a 96 % yield as a white foam.

Synthesis of compound **4**

A solution of HCl (gas; 1.0 M in ethyl acetate, 37 mL, 36.69 mmol) was added to a solution of **12** (389 mg, 0.25 mmol) and the reaction mixture was stirred at r. t. for 25 h. The resulting residue was filtrated using sintered glass funnel and washed with diethyl ether to furnish **4** as a white solid in a 95 % yield.

Procedure for preparation of compound **15**

Synthesis of compounds **13** and **14**

Sulfuryl chloride (13.5 g, 100 mmol) was added dropwise to an ice-cooled suspension of NaN_3 (6.5 g, 100 mmol) in acetonitrile (100 mL) resulting in a white salt formation (**13**). After stirring the mixture at r. t. overnight, it was cooled over an ice bath, and imidazole (12.9 g, 100 mmol)

was added in portion-wise and the resulting slurry was stirred at r. t. for 3 h. The initial addition of imidazole resulted in pinkish color which turned white upon complete addition. The mixture was diluted with ethyl acetate (200 mL) and H_2O (200 mL), and the aqueous layer was separated and discarded. The organic layer was washed with H_2O (200 mL), then with saturated aqueous $NaHCO_3$ (2 × 200 mL), dried over $MgSO_4$ and filtered. The yellow oily liquid **14** obtained after evaporating the solvent was used for the next step without further purification.

Synthesis of **14·H_2SO_4**

The reaction was carried out using a slightly modified literature procedure.[93,94] Sulfuric acid [93 % (w/w), 5.8 mL in diethyl ether (50 mL)] was added slowly to a solution of imidazole-1-sulfonyl azide **14** [100 mmol in diethyl ether (50 mL)] at 0 °C. The reaction mixture was stirred at r. t. for 30 min. The precipitate was filtered, washed with diethyl ether and dried in vacuum to give a white crystalline powder **14·H_2SO_4** with an 80 % yield.

Synthesis of compound **15**

Imidazole-1-sulfonyl azide hydrogen sulfate (**14·H_2SO_4**, 647 mg, 2.39 mmol) was added to a mixture of the commercially available N^1,N^4,N^9-*tris*(Boc)spermine (1.0 g, 1.99 mmol), K_2CO_3 (0.5 mmol) and $CuSO_4·5H_2O$ (5 mg, 0.02 mmol) in methanol (22 mL), and the resulting reaction mixture was stirred at r. t. for 30 h. It was diluted with H_2O (50 mL) and extracted with ethyl acetate (3 × 50 mL). After drying the organic layer over anhydrous Na_2SO_4, the volatiles were removed under reduced pressure. The crude product obtained after aqueous work up was column purified on silica gel using ethanol in chloroform [from 100/0 v/v (%) to 100/2 v/v (%)] to afford **15** in a 93 % yield as an oily liquid.

Results and discussion

Synthetic procedure

First, we discuss the synthesis of oleanolic acid-triazole-spermine conjugates **2**–**4** (Scheme 1). To design novel structures, we used Cu(I)-catalyzed Huisgen 1,3-dipolar cycloaddition reaction providing a facile route for 1,2,3-triazoles by selective functionalization of either hydroxyl group [C(3)-OH] or carboxylic acid group [C(17)-COOH].[95] Apart from the increased yield, the 1,4-disubstituted 1,2,3-triazoles also share certain similarities in their structural as well as physico-chemical properties with the amide bond.[96,97] The functionalization at C(3)-OH of **1** was achieved by carrying out the benzyl protection of carboxyl acid group and yielded **5**. The compound **5** was then reacted with propargyl bromide in the presence of sodium hydride in THF and **6** was obtained.[98] Simultaneously, *tert*-butoxy (Boc)-protected azide derivative of spermine derivative **15** was prepared according to the slightly modified literature procedures[93,94] (see Experimental section and the Scheme S1 in Supporting Information). Compound **6** upon *in situ* generated Cu(I)-catalyzed Huisgen 1,3-dipolar cycloaddition reaction[98] with **15** in DCM/H_2O at r. t. furnished **7**. Hydrogenation of **7** using 10 % Pd/C as a catalyst under H_2 atmosphere in a THF/EtOH mixture resulted in a deprotection of carboxylic acid, furnishing **8**. Acid hydrolysis of **8** using 1.0 M HCl (gas) in ethyl acetate[99] resulted in a preparation of **2**. Compound **3** was synthesized by reacting **1** with propargyl bromide in the presence of K_2CO_3 to furnish **9** in the first step. The ester **9** was then subjected to a series of transformation steps that include Cu(I)-catalyzed Huisgen 1,3-dipolar cycloaddition reaction to obtain **10**, followed by a removal of the Boc-protecting groups using 1.0 M HCl (gas) in ethyl acetate to get the conjugate **3**. To synthesize **4**, the intermediate **9** was reacted with propargyl bromide in the presence of sodium hydride to obtain **11**. Subsequently, Cu(I)-catalyzed Huisgen 1,3-dipolar cycloaddition reaction

was applied under the above described conditions, yielding **12**. A removal of the Boc-protecting groups, present in **12**, was carried out by 1.0 M HCl (gas) in ethyl acetate, furnishing **4**. A detailed synthetic and purification procedures are described in the Experimental section. The spectral data, 1D (^{1}H and ^{13}C), 2D NMR (^{1}H-^{13}C correlation spectroscopy), electrospray ionization MS, IR spectra and other related characterization of intermediate and target products are presented in Supporting Information (see also Figures S3-S15).

Gelation studies

The presence of the lipophilic core and the cationic spermine side chains impart amphiphilic nature to the conjugates **2** and **3**. The oleanolic acid core has an end to end length of 1.45 nm based on its solid-state structure, and the triazole linked spermine in its fully stretched conformation has a length of 1.97 nm (Figure 1 and Figure S1). Though **2** and **3** have a similar overall structure, they differ in the position of spermine substituents, i.e., they are positional isomers. The conjugate **2** has a free carboxylic acid group, whereas **3** has a free hydroxyl group. On the other hand, **4** has both these groups functionalized, resulting in a bolaamphiphile-like molecule. More importantly, oleanolic acid-triazole-spermine conjugates **2**–**4** differ from conventional surfactant molecules due to the conformationally rigid and chiral triterpenoid core. Natural bile salts (steroid compounds) and their synthetic derivatives are classical examples for this type of unconventional surfactants and are known for their unique aggregation behavior.[26-32] Depending on the number and position of hydroxyl groups and functional transformation, bile salts and their derivatives are known to form globules, tubules, and fibrous gel networks.[10,26-32] Therefore, it is desirable to investigate the self-assembly behavior of the novel amphiphilic building blocks based on the plant triterpenoid **1**. The solubility of **2**–**4** was tested in 23 different solvents (Table 1). Interestingly, **2** and **3** underwent gelation – mostly in polar protic solvents –

when tested at 1.0 % (note: from hereafter all percent values (%) are in w/v of gelator/solvent), as suggested by vial inversion test (we have used 1.0 % as an upper limit for gelation tests). Conjugate **2** was gelled at a concentration as low as 0.5 % in 1-butanol, and 1.0 % in 1-propanol, 2-propanol, 1-pentanol, 1-hexanol, 1-heptanol, and in polar aprotic solvents, pyridine and *N*,*N*-dimethylformamide (DMF). Similarly, gels were obtained for **3** in 2-propanol, 1-butanol, 1-pentanol, 1-heptanol, in polar aprotic solvents, pyridine, DMF, acetonitrile, and, surprisingly, in a non-polar solvent (1,4-dioxane) at a concentration of 1.0 %. The resulting gels were translucent or opaque, depending on the concentration and the type of organic solvent used for gelation (Figure 2). In all other tested organic solvents, both **2** and **3** remained in the solutions or precipitated after allowing to stand at r. t., or they remained insoluble (Table 1). However, **4** is either insoluble or remaining in a solution, no gelation was observed. This finding already suggests that the gelation is strongly affected by the number and position of the spermine units, as well as by the presence of the unconjugated hydroxyl or carboxylic acid groups. Driving force of the gel formation is connected with the presence of electrostatic interactions between a quaternary amino group present in the spermine chain and a chloride anion,[61] which is present in all three conjugates. However, intermolecular hydrogen bonds between the carbonyl and the amino groups represent an important factor when non-gelator property of **4** is taken into consideration in contrary to those of **2** and **3**.

Table 1. Solvents (non-polar, polar protic, polar aprotic, acid and bases) tested for gelation studies of **1**–**4** (gelation concentration c = 1.0 %).

Solvent / compound	**1**	**2**	**3**	**4**
benzene	I	I	I	I
chlorobenzene	S	SS	SS	I

toluene	PI	SS	I	I
carbon tetrachloride	PI	SS	SS	I
1,4-dioxane	S	P	OG	I
chloroform	S	SS	S	I
dichloromethane	PI	I	I	I
acetonitrile	P	P	OG	I
DMF	S	TG	TG	PI
DMSO	S	S	S	S
pyridine	S	pCG	CG	S
methanol	OG	S	S	S
1-propanol	OG	CG	VS	I
2-propanol	S	TG	OG	P
1-butanol	S	TG	OG	I
1-pentanol	S	TG	OG	PI
1-hexanol	S	pTG	VS	PI
1-heptanol	S	TG	OG	PI
1-octanol	S	P	P	I
formic acid	PI	S	S	S
triethylamine	S	I	P	I
N-methyl morpholine	S	I	I	I

Note. TG = Translucent gel, OG = opaque gel, pTG = partial translucent gel, pCG = partial clear gel, P = precipitated upon cooling, S = soluble at r. t., I = insoluble at boiling point, PI = partially soluble at boiling point, SS = suspension, VS = viscous solution.

Electron microscopy analysis

Scanning electron microscopy (SEM)

To investigate the structure of the supramolecular assemblies, we carried out EM (SEM or TEM) imaging of all the studied gels of **2** and **3** (Note: only representative micrographs are presented in main text). Ambient drying of gels (xerogels) resulted in film-like structures due to drying artifacts (Figure S16). Therefore, aerogels were prepared using liquid nitrogen freeze-drying technique (see Supporting Information for details). The SEM image of methanol gel of **1** (Figure 2a) showed microcrystalline structures (Figure 2). A representative SEM image of 0.5 % 1-butanol gel of **2** is shown in Figure 2e, displaying highly entangled fibrous networks with an average lateral dimension of 35 ± 5 nm and with indefinite length. To study the effect of concentration on morphology, SEM micrographs of 1-butanol gels of **2** at four different concentrations (0.5, 1.0, 1.5 and 2.0 %) were obtained (see Supporting Information, Figure S17). However, the fiber diameter changed slightly upon increasing the concentration, and, the fibers tend to be densely packed, (see Supporting Information, Figure S18, and Table S2), a property, that is consistent with the literature reports.[100] Moreover, for gels at higher concentrations, due to dense packing the determination of the lateral dimensions of individual fibers was challenging. In all the solvents tested for gelation, **2** showed similar morphological features with highly entangled network of fibers (Figure S16). A representative SEM micrograph from the 1,4-dioxane gel (1.0 %) of **3** with highly entangled fibrous networks is shown in Figure 2f. The fiber morphologies in aerogels of **3** are similar to those of **2**. However, the lateral dimensions of the fibers were different from those for **2**. For example, aerogels derived from DMF gels of **2** and **3** showed the lateral dimensions of 43 ± 5 nm and 29 ± 5 nm, respectively (see Supporting Information, Figure S19 and Table S3).

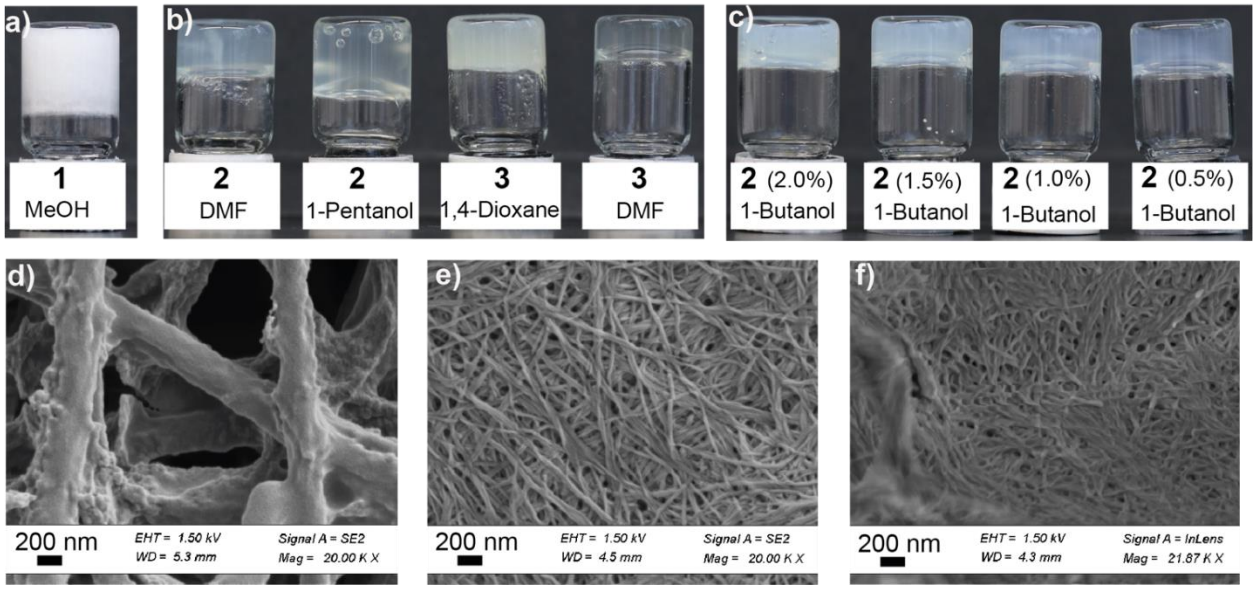

Figure 2. Gelation and scanning electron microscopy. Electron micrographs of representative gels a) **1** in methanol, 1.0 %, b) **2** and **3** in different solvents, 1.0 %, c) **2** in 1-butanol at different concentrations; d) SEM micrographs of methanol gel of **1**; e) SEM micrograph of freeze-dried 1-butanol gel of **2**, 0.5 %, and f) SEM micrograph of freeze-dried 1,4-dioxane gel of **3**, 1.0 %.

Transmission electron microscopy (TEM)

To obtain more information about fiber morphology, TEM imaging was performed for all gels (see Supporting Information for sample preparation). TEM micrographs of all the gels studied in this work showed the presence of fibrous networks. Figure 3 shows the representative TEM micrographs of 1-propanol gel of **2** (1.0 %) and 1-pentanol gel of **3** (1.0 %). More importantly, in some cases, the helical twist was observed (Figure 3b, 3d) with a pitch length of about 90 nm and lateral dimension varying from 15 to 25 nm (Figure 3e). The lateral dimensions observed under TEM imaging are comparable with the results obtained from SEM imaging. The TEM micrographs from all other gels are presented in Supporting Information (Figure S20).

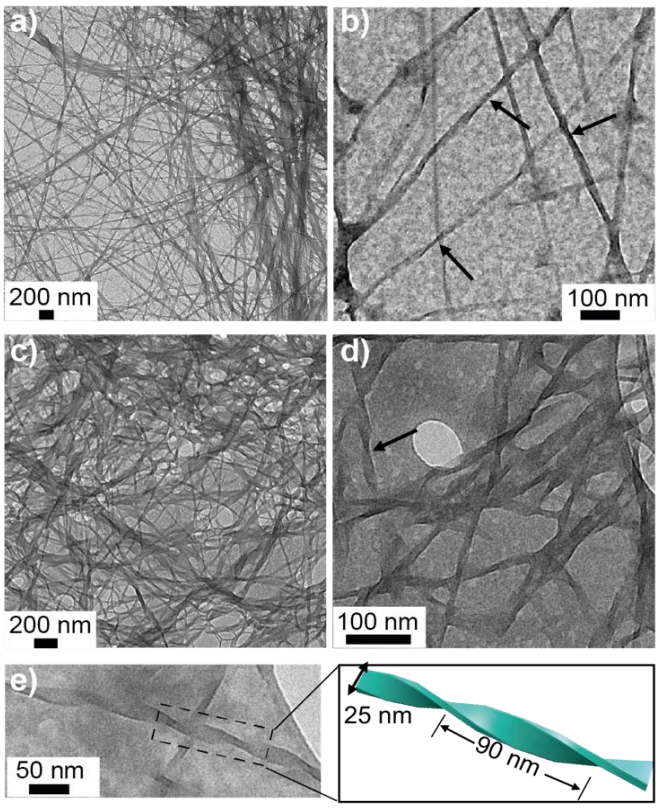

Figure 3. Transmission electron microscopy. a,b) TEM micrographs of 1.0 % 1-propanol gel of **2**; c,d) TEM micrographs of 1.0 % 1-pentanol gel of **3**; e) a single fiber with helical twist is shown (left) together with its graphical representation (right).

X-ray powder diffraction and thermal analysis

To further gain insights about solid state and thermal properties of the conjugates, thermogravimetric analysis (TGA), differential scanning calorimetry (DSC) and X-ray powder diffraction (XRPD) studies of oleanolic acid (**1**), synthetic solid compounds **2**–**4**, but aerogels from 1-butanol gel of **2** (1.0 %) and 1-pentanol gel of **3** (1.0 %) were performed (see Supporting

Information for experimental details and results). TGA and DSC results revealed a decreased decomposition temperature for the conjugates and the aerogels compared to parent **1** (see Supporting Information, Table S4, Figures S21, S22). XRPD studies revealed the semi-crystalline nature of **1**. However, the target conjugates **2**–**4** showed broad featureless patterns in their powder X-ray patterns (see Supporting Information, Figure S23). These results suggest that the synthetic solids as well as the self-assembled nanostructures in gels are amorphous.

Mechanical properties of gels

For rheological measurements, only those gels that are suitable for repeated rheological measurements were used that can be transferred onto the rheometer without losing their structures. Accordingly, pre-made and stabilized 1-propanol, 2-propanol, 1-butanol and 1-heptanol gels of **2** were studied (Figure 4, see also Supporting Information for Experimental details). The gels have already shown that the storage modulus (G') is several folds higher than that of loss modulus (G") suggesting that the systems under investigation are already in gel state (viscoelastic) and remained constant under time sweep (30 min) experiments (Figure 4a). The storage modulus (G') of gels varies as a function of the frequency under frequency sweep experiment (Figure 4b). The frequency sweep experiment provides insights into the nature and lifetime of the bonds that are involved in network junctions.[101] The frequency dependence of the storage and elastic moduli observed for gels derived from **2** and **3** indicates the presence of junction networks and temporary bonds that form the networks. Such temporary bonds are sensitive to the frequency of the mechanical stress and the lifetime of the bonds. Our results suggest that there are junction networks as supported by SEM and TEM micrographs (Figures 2 and 3). At a given concentration the stiffness of the gels varied in the following order, 1-butanol > 1-propanol > 2-propanol > 1-heptanol with G' values of 1.4 kPa, 0.7 kPa, 0.5 kPa, and 0.025

kPa, respectively (see Supporting Information, Figure S24c1). For a given solvent, the modulus was increased as a function of concentration, a property that is typical for low molecular weight gelators. Figure 4e, 4f shows the concentration dependent, stress and strain sweep experiments for 1-butanol gels of **2** (for time and frequency sweep experiments see Supporting Information, Figure S24a, S24b). For 1-butanol gels of **2**, the storage modulus was increased from 0.22 kPa for 0.5 % to 6.5 kPa for 2.0 %, which is a 30-fold increase in the stiffness (see Supporting Information, Figure S24c2). Yield stress values were determined by tangent analysis method. The yield stress values of 1-butanol, 1-propanol, 2-propanol, and 1-heptanol gels of **2** were found to be 30, 24, 13 and 8 Pa, respectively (Figure 4c). Similarly, yield stress values for 1-butanol gels of **2** at different concentrations were determined as 3, 16, 40 and 95 Pa for 0.5, 1.0, 1.5 and 2.0 %, respectively (Figure 4f). For compound **3**, gels that are suitable for rheological measurements were obtained from 1-pentanol and 1-heptanol. Time, frequency, strain, and stress sweep experiments were performed for 1-heptanol and 1-pentanol gels of **3** and the details are presented in Supporting Information, Figure S24. For 1.0 % gels, G' values were found to be 1.4 kPa and 0.3 kPa for 1-pentanol and 1-heptanol, respectively. The only common solvent for rheological measurements of **2** and **3** was 1-heptanol, in which both compounds formed gel that could be transferred onto the rheometer without losing its structure. The storage modulus of 1.0 % 1-heptanol gel was found to be 0.025 kPa (for **2**), and 0.95 kPa (for **3**), respectively (see Supporting Information, Figure S24c1, S24d). The yield stress values of 1-pentanol and 1-heptanol gels of **3** were found to be 51 Pa and 35 Pa, respectively (see Supporting Information, Figure S24f). These results show us that **2** forms stronger gel than **3** in alcoholic solvents, in general. Furthermore, the stiffness of gels decreases with increasing number of carbon atoms in the alcoholic solvents. The structure of these carbon chains present in alcoholic solvents, i.e.,

whether they are branched or linear, has also an impact on stiffness of gels. Linear chains-bearing alcoholic solvents seem to form more stiffed gels than the alcoholic solvents with branched carbon chains. Therefore, to induce gelation, a delicate balance exists between carbon chain length and its structural property in the used alcohols.

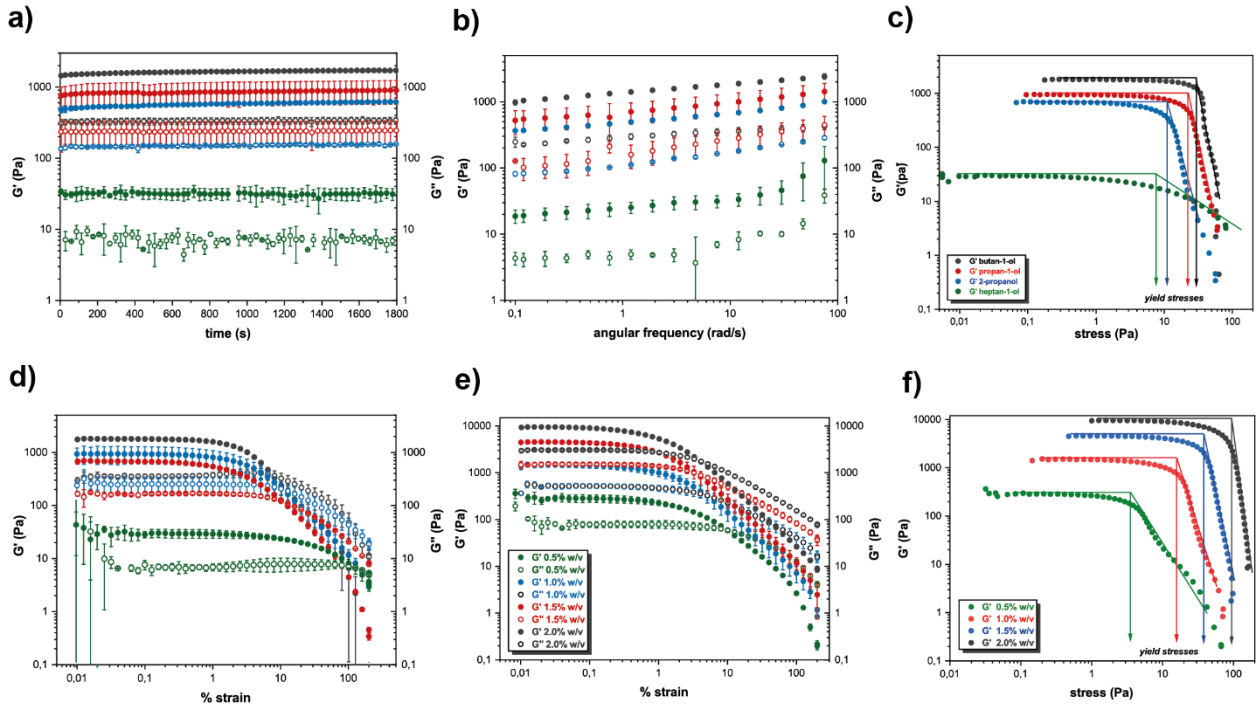

Figure 4. Rheological properties of gels. a) Time sweep experiments of gels derived from **2**, b) frequency sweep experiments of gels derived from **2**, c) stress sweep experiments derived from **2**, d) strain sweep experiments derived from **2** [(full circles indicate G', empty circles indicate G'', 1-butanol gel (black), 1-propanol gel (red), 2-propanol gel (blue), 1-heptanol gel (green)], e),f) the effect of concentration on mechanical properties of 1-butanol gel of **2**.

Self-healing properties

Step-strain rheological measurements were performed to investigate the reversible gel ⇔ sol transition and self-recovery, under several cycles. For the step-strain experiments, controlled

strains of 0.1 % and 150 % were applied for 60 s, respectively. The gels showed an immediate response to increased strain by turning into sol indicated by the rapid decrease in G' by several folds and well below that of G" (Figure 5a). The application of increased strain also appears to break the structure further during the 60 s experiment as shown by the gradually decreasing elastic moduli values in the subsequent cycles. The gels recovered their original mechanical strength almost instantaneously upon switching to lower strain (0.1 %) i.e. rapid self-recovery. Importantly, the process can be repeated for several cycles. However, slightly lower G' was observed after the first high–low strain cycle, which remained constant in subsequent cycles, a property typically observed for several low molecular weight gelators. Importantly, the gels were able to recover up to 96 % of their original storage moduli even after four cycles. The percentage recovery of storage moduli of 1-butanol, 1-propanol, and 2-propanol gels of **2** was found to be 96, 89 and 78 %, respectively (Figure 5a, see also Supporting Information and Figure S25 for other gels of **2** and **3**). Similarly, for 1-pentanol and 1-heptanol gels of **3**, the percentage recovery of the original storage moduli was found to be 76 and 75 %, respectively.

Thixotropic properties

To evaluate the thixotropic property of gels of **2** and **3**, their flow curves were also measured (Figure 5b, 5c). The measurement was carried out as follows: the shear stress was measured while increasing the shear rate from 0 to 100 s^{-1} and then decreased back to 0 s^{-1}. Figure 5b and 5c shows change in the viscosity and shear stress as a function of shear rate for 2-propanol gel (1.0 %) of **2** and 1-pentanol gel (1.0 %) of **3**, respectively. A clear hysteresis loop showing a clockwise turn was observed suggesting the gels under investigation display thixotropic property.

At macroscopic level, by manual shaking, the gel resulted in a gel ⇔ sol transition recovering within 60 seconds, showing a rapid recovery. Figure 5d and 5e shows selected snapshots of 1-butanol gel (1.0 %) of **2**, demonstrating a rapid recovery and thixotropic properties by either shaking or vortexing (see video S1). Thixotropic nature of gels can be explained on the basis of the amorphous fibrous network. X-ray diffraction studies of the aerogels suggest the amorphous nature of the gel network (Figure S23). This observation is in agreement with other thixotropic gels reported in the literature.[54-56]

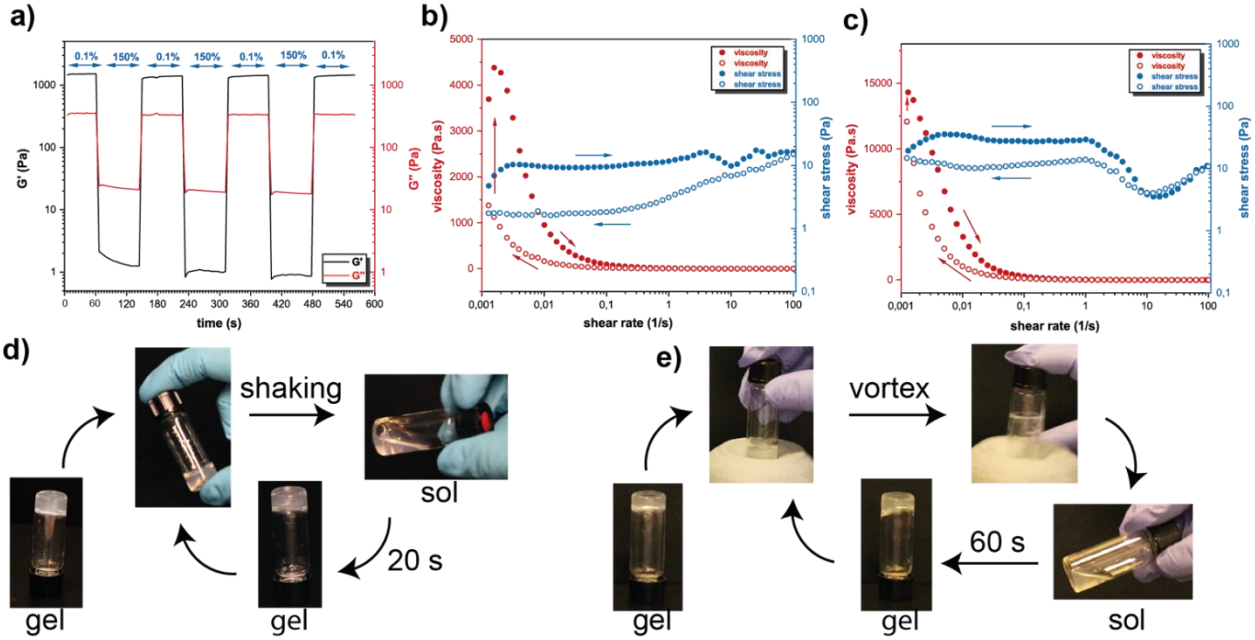

Figure 5. Self-recovery and thixotropic properties. a) Step-strain experiments showing self-healing properties of 1-butanol gel of **2**, flow tests showing viscosity *v/s* shear rate and shear stress *v/s* shear rate for b) 2-propanol gel of **2** and c) for 1-pentanol gel of **3**, d, e) snapshots from video demonstrating thixotropy by manual shaking and vortexing of 1-butanol gel of **2**.

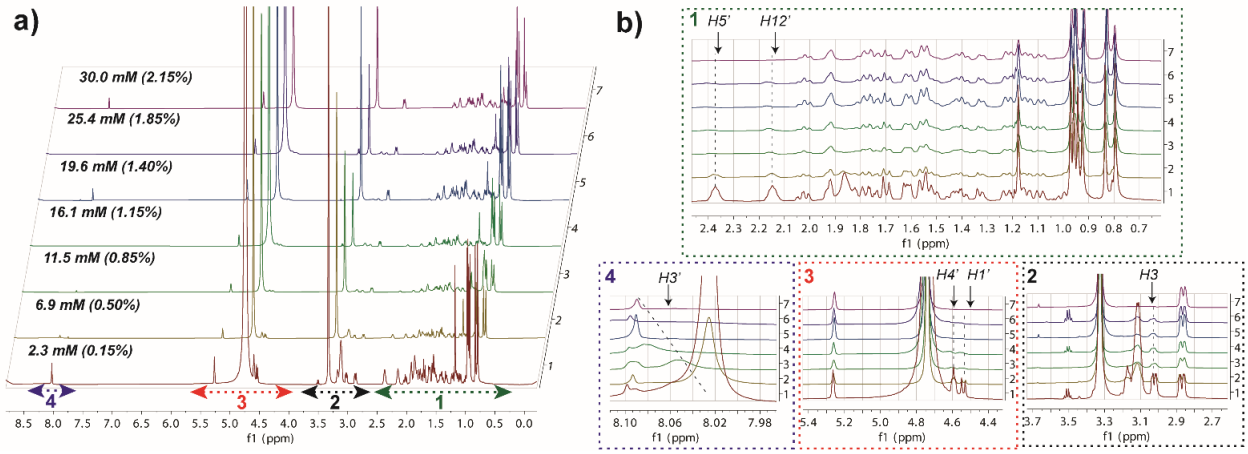

Figure 6. VC ^{1}H-NMR graph of a) **2** in CD_3OD at 40°C, b) expanded version of VC ^{1}H-NMR graph of **2** in 4 different regions (right).

VC and VT ^{1}H NMR

The VC ^{1}H NMR spectra of **2**–**4** in CD_3OD at 40°C (to mimic the conditions of gel preparation) were measured to gain insights into the interactions involved in self-assembly. The reason why CD_3OD was chosen for the VC ^{1}H-NMR spectra measurements was the observation of a gel even at a concentration as low as 0.5 % in the NMR tube when used other solvents than CD_3OD, e.g., DMF. Because **2** and **3** form gels mostly in alcoholic solvents, this finding prompted us to check their behavior in CD_3OD. Relatively sharp ^{1}H NMR resonance peaks, which arise presumably from the non-aggregated molecules, were observed at a low concentration for **2**–**4**. As the concentration increased, the peaks turned to become broader or even remained NMR silent with a slight downfield shift. The broadening, along with the invisible nature of certain signals is possibly due to a self-assembly of **2**–**4**. Figure 6 shows the VC ^{1}H NMR spectrum in a concentration range from 0.15 % to 2.15 % of **2** (see Supporting

Information, Figure S26 for **3** and **4**). The signal broadening is more pronounced for **2** compared to that of **3** and **4**. The fact that certain NMR signals turned to become NMR silent above certain concentration is attributed to the large size of the aggregates. The VT ^{1}H NMR spectra of **2**–**4** were also measured to see the effect of temperature on aggregates. However, the maximal temperature limit of 40 °C can be reached when CD_3OD used as an NMR solvent, due to its boiling point. As a consequence of this maximum temperature limitation, the ^{1}H NMR experiments carried out accordingly, revealed no important information about aggregates. In other words, no changes in the chemical shift values of the ^{1}H NMR resonance peaks were observed (see Supporting Information, Figure S27).

IR spectroscopy

Inter- and intramolecular interactions can be investigated using IR spectroscopy, which is frequently used technique in gel studies. With the aim to better understand the driving forces leading to the gel formation, IR spectra of the aerogels prepared from **2** and **3** in different solvents were measured. The spectra of aerogels were compared with those of the corresponding synthetic solids in their powder form (see Supporting Information, Figure S28). The IR spectra of the aerogels, as well as those of the synthetic solids exhibited similar characteristic peaks. This finding suggests that the molecular structure in the gel state resembles that of the synthetic powder form. These findings are in agreement with the XRD results. In addition, no spectral differences were observed in the IR spectra when aerogels, prepared in different solvents, were compared. This result is in agreement with the SEM and TEM micrographs, in which similar entangled fibrous networks were obtained in each solvent used for the gels preparation. This type of observation has already been described for steroidal gelators in the literature,[58] however, it is a novel knowledge found with the triterpenoid-based gelators described here.

Cytotoxicity

The target compounds **2**–**4** showed cytotoxicity in the four tested cancer cell lines (Table 2; for experimental details See Supporting Information). CDDP (cisplatin) was used as a positive reference compound. An important difference was observed in the cytotoxicity values of **2** in comparison with those of **3** and **4**. It seems that the location and number of the spermine units on the triterpenoid skeleton plays a key role for cytotoxicity. Substitution of the C(17)-COOH group with the spermine substituent in **3** (C(3)-OH group remains free) and in **4** led to the one order increase of cytotoxicity in comparison with the data obtained for **2**. Surprisingly, high cytotoxicity was found in tests of **4** in malignant melanoma cells (G-361). Melanoma cancer belongs among the most aggressive cancer types. Even though **3–4** were toxic towards human fibroblasts, they still exhibited better cytotoxicity profile than CDDP (a positive control) against several cancer cell lines (**3** against MCF7 and Hela, and **4** against MCF7, Hela and G-361).

Table 2. Cytotoxicity (IC_{50} [μM]) of **2**–**4** in four cancer cell lines and normal human fibroblasts after 72 h.

Compound	MW	Cytotoxicity (IC_{50} [μM]; 72 h)				
		CEM	MCF7	HeLa	G-361	BJ
2	723	29.8 ± 3.3	28.0 ± 1.0	12.6 ± 2.8	27.8 ± 0.9	14.2 ± 0.4
3	723	2.1 ± 0.8	**3.7 ± 1.0**	**3.7 ± 0.5**	6.6 ± 0.4	2.3 ± 0.1
4	989	7.1 ± 1.1	**2.7 ± 0.7**	**2.2 ± 0.1**	**0.8 ± 0.0**	1.9 ± 0.0
CDDP [a]	300.05	0.8 ± 0.1	7.7 ± 1.7	11.4 ± 3.8	4.5 ± 0.6	6.9 ± 0.9

[a] *cis*-Diamminedichloridoplatinum(II) (cisplatin), a pharmacologically used agent for treating different cancer types, a positive reference compound.

Conclusion

Our results showed that modifications of triterpenoids allow the rational design of novel building blocks with unique self-assembly and material properties. The synthetic approach presented here supports that Cu(I)-catalyzed Huisgen 1,3-dipolar cycloaddition represents a convenient synthetic method for the facile chemical transformation of sterically hindered functional groups of triterpenoids. In this study compounds **2**–**4** were synthesized starting from **1** and their structure was characterized. Conjugates **2** and **3** exhibited solvent dependent self-assembly resulting in thixotropic and self-healing organogels with helical fibrous networks. Gelation properties of the studied compounds were affected by the position and the number of the spermine units. Bolaamphiphile-like compound **4** was found to be a non-gelator, and displayed different behavior than **2** and **3** that were found to be gelators. Gels obtained from **2** and **3** exhibited different stiffness values. Our results suggest that the structural modification of gelator and the solvents significantly affect gelation and mechanical properties of gels. The gels, xerogels and aerogels, were characterized using multiple and complimentary microscopic and spectroscopic methods. Further, mechanical property of gels was extensively studied using oscillatory rheological measurements.

Cytotoxicity of **2**–**4** was tested in four different cancer cell lines within this investigation. The cytotoxicity depends on the way of substitution of the oleanolic acid with the spermine side chains. Importantly, compounds bearing spermine as a substituent in the C(17)-COOH group, i.e., **3** and **4**, showed higher cytotoxicity. Furthermore, **3** (against MCF7 and HeLa) and **4** (against MCF7, HeLa and G-361) showed somewhat improved cytotoxicity profile compared to that of positive control CDDP.

Overall, this work shows that there is a potential to utilize naturally abundant sustainable oleanolic acid for new functional materials, and this approach can be extended to other triterpenoids. More importantly, this work also opens possibilities to theoretical and computational chemists to investigate the self-assembly of this new class of amphiphiles. Each partial investigation in this work contributed to a formation of a complex view on characteristics of the studied supramolecular systems with the ability to form supramolecular gels exhibiting a potential to become promising next-generation materials for a broad range of technical and biomedical applications.

ASSOCIATED CONTENT

Supporting Information.

The following file is available free of charge.

Supporting Information brings additional details on the analytical data of the prepared compounds, on gelation studies, SEM, TEM, rheology studies, VC and VT NMR spectra, IR spectra, powder diffraction analysis, TG/DSG analysis and *in silico* energy calculations (PDF).

AUTHOR INFORMATION

Corresponding Authors

Nonappa – Aalto University, Department of Applied Physics, Puumiehenkuja 2, FI-02150 Espoo, Finland and Tampere University, Faculty of Engineering and Natural Sciences, P.O. Box

541, FI-33101 Tampere, Finland. Email: Email: nonappa@aalto.fi; nonappa.nonappa@tuni.fi; ORCID ID: 0000-0002-6804-4128.

Zdeněk Wimmer – University of Chemistry and Technology in Prague, Department of Chemistry of Natural Compounds, Technická 5, 16028 Prague 6, Czech Republic and Institute of Experimental Botany of the Czech Academy of Sciences, Isotope Laboratory, Vídeňská 1083, 14220, Prague 4, Czech Republic. E-mail: zdenek.wimmer@vscht.cz; wimmer@biomed.cas.cz; ORCID ID: 0000-0002-4512-0116.

Authors

Zulal Özdemir – University of Chemistry and Technology in Prague, Department of Chemistry of Natural Compounds, Technická 5, 16028 Prague 6, Czech Republic and Institute of Experimental Botany of the Czech Academy of Sciences, Isotope Laboratory, Vídeňská 1083, 14220, Prague 4, Czech Republic. E-mail: zulalozdemr@gmail.com; ORCID ID: 0000-0002-9083-4919.

David Šaman – Institute of Organic Chemistry and Biochemistry of the Czech Academy of Sciences, Flemingovo náměstí 2, 16610 Prague 6, Czech Republic. E-mail: nmrsaman@gmail.com. ORCID ID: 0000-0001-5578-1930.

Kia Bertula – Aalto University, Department of Applied Physics, Puumiehenkuja 2, FI-02150 Espoo, Finland. E-mail: kia.bertula@aalto.fi; ORCID ID: 0000-0002-7134-3591.

Manu Lahtinen – University of Jyväskylä, Department of Chemistry, P. O. Box. 35, FI-40014 Jyväskylä, Finland. E-mail: manu.k.lahtinen@jyu.fi; ORCID ID: 0000-0001-5561-3259.

Lucie Bednárová – Institute of Organic Chemistry and Biochemistry of the Czech Academy of Sciences, Flemingovo náměstí 2, 16610 Prague 6, Czech Republic. E-mail: bednarova@uochb.cas.cz; ORCID ID: 0000-0003-3367-0193.

Markéta Pazderková – Institute of Organic Chemistry and Biochemistry of the Czech Academy of Sciences, Flemingovo náměstí 2, 16610 Prague 6, Czech Republic and Charles University, Institute of Physics, Faculty of Mathematics and Physics, Ke Karlovu 5, 12116 Prague 2, Czech Republic. E-mail: marketha@gmail.com; ORCID ID: 0000-0003-1086-4497.

Lucie Rárová – Laboratory of Growth Regulators, Institute of Experimental Botany of the Czech Academy of Sciences, and Faculty of Science, Palacký University, Šlechtitelů 27, CZ-78371 Olomouc, Czech Republic. E-mail: lucie.rarova@upol.cz; ORCID ID: 0000-0002-3300-007X.

Author Contributions

The manuscript was written through contributions of all authors. All authors have given approval to the final version of the manuscript. ‡ D.Š., K.B., M.L., L.B. and M.P. contributed to different analytical methods.

Notes

The authors declare no competing financial interest.

ACKNOWLEDGMENT

The authors thank for funding of this research through the grants from MPO: FV10599 (Z.Ö.) and FV30300 (Z.W.). We acknowledge the provision of facilities and technical support by Aalto University Nanomicroscopy Center (Aalto-NMC). We thank Dr. S. Hietala for useful discussion on rheology. Part of this work is also carried out under the framework of Centre of Excellence in Molecular Engineering of Biosynthetic Hybrid Materials (HYBER 2014-2019) and Photonics Research and Innovation (PRIEN) flagship program. Z.Ö. thanks Erasmus+ program of the EU for funding her study visit to the Aalto University, Finland. L.R. thanks the Czech Science Foundation for the grant No. 19-01383S.

ABBREVIATIONS

DCM, dichloromethane; DMF, *N*,*N*-dimethylformamide; THF, tetrahydrofuran; TBTA, *tris*[(1-benzyl-1*H*-1,2,3-triazol-4-yl)methyl]amine; TLC, thin layer chromatography; CEM, T-lymphoblastic leukemia; MCF7, breast carcinoma; HeLa, cervical carcinoma; G-361, malignant melanoma; BJ, human foreskin fibroblasts.

REFERENCES

(1) Weiss, R.G. Molecular Gels: Structure and Dynamics, Royal Society of Chemistry, Cambridge, **2018**, pp. 1–376.

(2) Chivers, P. R. A.; Smith, D. K. Shaping and structuring supramolecular gels. *Nat. Rev. Mater.* **2019**, *4*, 463–478.

(3) Weiss, R. G. The Past, Present, and Future of Molecular Gels. What Is the Status of the Field, and Where Is It Going? *J. Am. Chem. Soc.* **2014**, *136*, 7519–7530.

(4) Weiss, R. G.; Terech, P. Molecular Gels: Materials with Self-Assembled Fibrillar Networks, Springer, Netherlands, **2006**, pp. 1–938.

(5) Escuder, B.; Miravet J. F. in Functional Molecular Gels, The Design of Molecular Gelators, (Eds.: Zweep, N.; van Esh, J. H.), Royal Society of Chemistry, Cambridge, **2013**, pp. 1–29.

(6) Kuroiwa, K.; Shibata, T.; Takada, A.; Nemoto, N.; Kimizuka, N. Heat-Set Gel-like Networks of Lipophilic Co(II) Triazole Complexes in Organic Media and Their Thermochromic Structural Transitions. *J. Am. Chem. Soc.* **2004**, *126*, 2016.

(7) Xie, F.; Qin, L.; Liu, M. A dual thermal and photo-switchable shrinking–swelling supramolecular peptide dendron gel. *Chem. Commun.* **2016**, *52*, 930–933.

(8) Ma, X.; Cui, Y.; Liu, S.; Wu, J. **A** thermo-responsive supramolecular gel and its luminescence enhancement induced by rare earth Y^{3+}. *Soft Matter* **2017**, *13*, 8027–8030.

(9) Zheng, Y.; Wang, D.; Cui, J.; Mezger, M.; Auernhammer, G. K.; Koynov, K.; H.-J. Butt, H.-J.; Ikeda, T. Redox-Responsive and Thermoresponsive Supramolecular Nanosheet Gels with High Young's Moduli. *Macromol. Rapid Commun.* **2018**, *39*, 1800282.

(10) Banerjee, S.; Das, R. K.; Maitra, U. Supramolecular gels 'in action'. *J. Mater. Chem.* **2009**, *19*, 6649–6687.

(11) Ke, H.; Yang, L.-P.; Xie, M.; Chen, Z.; Yao, H.; Jiang, W. Shear-induced assembly of a transient yet highly stretchable hydrogel based on pseudopolyrotaxanes. *Nat. Chem.* **2019**, *11*, 470–477.

(12) Zhang, M.; Xu, D.; Yan, X.; Chen, J.; Dong, S.; Zheng, B.; Huang, F. Self-Healing Supramolecular Gels Formed by Crown Ether Based Host–Guest Interactions. *Angew. Chem. Int. Ed.* **2012**, *51*, 7011–7015.

(13) Dastidar, P. Designing Supramolecular Gelators: Challenges, Frustrations, and Hopes. *Gels* **2019**, *5*, 15.

(14) Berthier, D.; Buffeteau, T.; Leger, J.-M.; Oda, R.; Huc, I. From Chiral Counterions to Twisted Membranes. *J. Am. Chem. Soc.* **2002**, *124*, 13486–13494.

(15) Mihajlovic, M.; Staropoli, M.; Appavou, M.-S.; Wyss, H. M.; Pyckhout-Hintzen, W.; Sijbesma, R. P. Tough Supramolecular Hydrogel Based on Strong Hydrophobic Interactions in a Multiblock Segmented Copolymer. *Macromolecules* **2017**, *50*, 3333–3346.

(16) Abdallah, D. J.; Weiss, R. G. *n*-Alkanes Gel n-Alkanes (and Many Other Organic Liquids). *Langmuir* **2000**, *16*, 352–355.

(17) Suzuki, M.; Nakajima, Y.; Yumoto, M.; Kimura, M.; Shirai, H.; Hanabusa, K. Effects of Hydrogen Bonding and van der Waals Interactions on Organogelation Using Designed Low-Molecular-Weight Gelators and Gel Formation at Room Temperature. *Langmuir* **2003**, *19*, 8622–8624.

(18) Das, R. K.; Banerjee, S.; Raffy, G.; Guerzo, A. D.; Desvergne, J.-P.; Maitra, U. Spectroscopic, microscopic and first rheological investigations in chargetransfer interaction induced organogels. *J. Mater. Chem.* **2010**, *20*, 7227–7235.

(19) Tatikonda, R.; Bertula, K.; Nonappa; Hietala, S.; Rissanen, K.; Haukka, M. Bipyridine based metallogels: an unprecedented difference in photochemical and chemical reduction in the in situ nanoparticle formation. *Dalton Trans.* **2017**, *46*, 2793–2802.

(20) Tatikonda, R.; Bulatov, E.; Özdemir, Z.; Nonappa; Haukka, M. Infinite Coordination Polymer Networks: Metallogelation of Aminopyridine Conjugates and in situ Silver Nanoparticle Formation. *Soft Matter* **2019**, *15*, 442–451.

(21) Cametti, M.; Džolić, Z. New frontiers in hybrid materials: noble metal nanoparticles – supramolecular gel systems. *Chem. Commun.* **2014**, *50*, 8273–8286.

(22) Meazza, L.; Foster, J. A.; Fucke, K.; Metrangolo, P.; Resnati, G.; Steed, J.W. Halogen-bonding-triggered supramolecular gel formation. *Nat. Chem.* **2013**, *5*, 42–47.

(23) Arnedo-Sánchez, L.; Nonappa; Bhowmik, S.; Hietala, S.; Puttreddy, R.; Lahtinen, M.; De Cola, L.; Rissanen, K. Rapid self-healing and anion selectivity in metallosupramolecular gels assisted by fluorine–fluorine interactions. *Dalton Trans.* **2017**, *46*, 7309–7316.

(24) Kolari, K.; Bulatov, E.; Tatikonda, R.; Bertula, K.; Kalenius, E.; Nonappa; Haukka, M. Self-healing, luminescent metallogelation driven by synergistic metallophilic and fluorine–fluorine interactions. *Soft Matter* **2020**, *16*, 2795–2802.

(25) Muraoka, T.; Cui, H.; Stupp, S. I. Quadruple Helix Formation of a Photoresponsive Peptide Amphiphile and Its Light-Triggered Dissociation into Single Fibers. *J. Am. Chem. Soc.* **2008**, *130*, 2946–2947.

(26) Tamminen, J.; Kolehmainen, E. Bile Acids as Building Blocks of Supramolecular Hosts. *Molecules* **2001**, *6*, 21–46.

(27) Virtanen, E.; Kolehmainen, E. Use of Bile Acids in Pharmacological and Supramolecular Applications. *Eur. J. Org. Chem.* **2004**, *16*, 3385–3399.

(28) Mukhopadhyay, S.; Maitra, U.; Krishnamoorthy, I. G.; Schmidt, J.; Talmon, Y. Structure and Dynamics of a Molecular Hydrogel Derived from a Tripodal Cholamide. *J. Am. Chem. Soc.* **2004**, *126*, 15905–15914.

(29) Nonappa; Maitra, U. Unlocking the potential of bile acids in synthesis, supramolecular/materials chemistry and nanoscience. *Org. Biomol. Chem.* **2008**, *6*, 657–669.

(30) Svobodová, H.; Noponen, V.; Kolehmainen, E.; Sievänen, E. Recent Advances in Steroidal Supramolecular Gels. *RSC Adv.* **2012**, *2*, 4985–5007.

(31) Zheng, M.; Strandman, S.; Waldron, K. C.; Zhu, X. X. Supramolecular hydrogelation with bile acid derivatives: structures, properties and applications. *J. Mater. Chem. B* **2016**, *4*, 7506–7520.

(32) Zheng, M.; Fives, C.; Waldron, K. C.; Zhu, X. X. Self-Assembly of a Bile Acid Dimer in Aqueous Solutions: From Nanofibers to Nematic Hydrogels. *Langmuir* **2017**, *33*, 1084–1089.

(33) Grassi, S.; Carretti, E.; Dei, L.; Branham, C. W.; Kahr, B.; Weiss, R. G. D-Sorbitol, a structurally simple, low molecular-mass gelator. *New J. Chem.* **2011**, *35*, 445–452.

(34) Sasselli, I. R.; Halling, P. J.; Ulijn, R. V.; T. Tuttle, T. Supramolecular Fibers in Gels Can Be at Thermodynamic Equilibrium: A Simple Packing Model Reveals Preferential Fibril Formation versus Crystallization. *ACS Nano* **2016**, *10*, 2661−2668.

(35) de Jong, J. J. D.; Lucas, L. N.; Kellogg, R. M.; van Esch, J. H.; Feringa, B. L. Reversible Optical Transcription of Supramolecular Chirality into Molecular Chirality. *Science* **2004**, *304*, 278−281.

(36) Terech, P. Metastability and Sol Phases: Two Keys for the Future of Molecular Gels? *Langmuir* **2009**, *25*, 8370−8372.

(37) Wang, Y.; Tang, L.; Yu, J. Investigation of Spontaneous Transition from Low-Molecular-Weight Hydrogel into Macroscopic Crystals. *Cryst. Growth Des.* **2008**, *8*, 884−889.

(38) De Rudder, J.; Bergé, B.; Berghmans, H. Competition between Gelation and Crystallization in Solutions of Syndiotactic Polystyrene in cis-Decalin. *Macromol. Chem. Phys.* **2002**, *203*, 2083−2088.

(39) Shimizu, T.; Masuda, M.; Minamikawa, H. Supramolecular Nanotube Architectures Based on Amphiphilic Molecules. *Chem. Rev.* **2005**, *105*, 1401–1443.

(40) Ziserman, L.; Lee, H.-Y.; Raghavan, S. R.; Mor, A.; Danino, D. Unraveling the Mechanism of Nanotube Formation by Chiral Self-Assembly of Amphiphiles. *J. Amer. Chem. Soc.* **2011**, *133*, 2511–2517.

(41) Oliveira, I. S.; Lo, M.; Araujo, M. J.; Marques, E. F. Temperature-responsive self-assembled nanostructures from lysine-based surfactants with high chain length asymmetry: from tubules and helical ribbons to micelles and vesicles. *Soft Matter* **2019**, *15*, 3700–3711.

(42) Palmans, A. R. A.; Meijer, E. W. Amplification of Chirality in Dynamic Supramolecular Aggregates. *Angew. Chem. Int. Ed.* **2007**, *46*, 8948–8968.

(43) Li, Z.-T.; Zhao, X. 'Scanning Electron Microscopy' in Supramolecular Chemistry: From Molecules to Nanomaterials, Vol. 2 – Techniques, (Eds.: Gale, P. A.; Steed, J. W.), John Wiley & Sons, Chichester, **2012**, pp. 619–631.

(44) Kikuchi, J.-I.; Yasuhara, K. in Supramolecular Chemistry: From Molecules to Nanomaterials, Vol. 2 – Techniques, (Eds.: Gale, P. A.; Steed, J. W.), John Wiley & Sons, Chichester, **2012**, pp. 633–645.

(45) Mallia, V. A.; R. G. Weiss, R. G. Correlations between thixotropic and structural properties of molecular gels with crystalline networks. *Soft Matter* **2016**, *12*, 3665–3676.

(46) Dawn, A.; Kumari, H. Low Molecular WeightSupramolecularGels Under Shear: Rheologyasthe Tool for Elucidating Structure–Function Correlation. *Chem. Eur. J.* **2018**, *24*, 762–776.

(47) Wool, R. P. Self-healing materials: a review. *Soft Matter* **2008**, *4*, 400–408.

(48) Hager, M. D.; Greil, P.; Leyens, C.; Zwaag, S. V. D.; Schubert, U. S. Self-Healing Materials. *Adv. Mater.* **2010**, *22*, 5424–5430.

(49) Yu, X.; Cao, X.; Chen, L.; Lan, H.; Liu, B.; Yi, T. Thixotropic and self-healing triggered reversible rheology switching in a peptide-based organogel with a cross-linked nano-ring pattern. *Soft Matter* **2012**, *8*, 3329–3334.

(50) Strandman, S.; Zhu, X. X. Self-Healing Supramolecular Hydrogels Based on Reversible Physical Interactions. *Gels* **2016**, *2*, 16.

(51) Bauer, W. H.; Collins, E. A. in Rheology: Theory and Application, (Ed.: Eirich, F. R.), Academic Press, New York, **1967**, ch. 8.

(52) Larson, R. G.; Wei, Y. A review of thixotropy and its rheological modeling. *J. Rheol.* **2019**, *63*, 477–501.

(53) IUPAC, (Ed.: McNaught, A. W. A. D.), Blackwell Scientific, Hoboken, NJ, **1997**.

(54) Weng, W.; Jamieson, A. M.; Rowan, S. J. Structural origin of the thixotropic behavior of a class of metallosupramolecular gels. *Tetrahedron* **2007**, *63*, 7419–7431.

(55) Mukhopadhyay, P.; Fujita, N.; Takada, A.; Kishida, T.; Shirakawa, M.; Shinkai, S. Regulation of a Real-Time Self-Healing Process in Organogel Tissues by Molecular Adhesives. *Angew. Chem. Int. Ed.* **2010**, *49*, 6338–6342.

(56) Lescanne, M.; Grondin, P.; D'Aléo, A.; Fages, F.; Pozzo, J.-L.; Monval, O. M.; Reinheimer, P.; Colin, A. Thixotropic Organogels Based on a Simple N-Hydroxyalkyl Amide: Rheological and Aging Properties. *Langmuir* **2004**, *20*, 3032–3041.

(57) Suzuki, M.; Hayakawa, Y.; Hanabusa, K. Thixotropic Supramolecular Gel Based on L-Lysine Derivatives. *Gels* **2015**, *1*, 81–93.

(58) Nonappa; Maitra, U. Simple esters of cholic acid as potent organogelators: direct imaging of the collapse of SAFINs. *Soft Matter* **2007**, *3*, 1428–1433.

(59) Ikonen, S.; Nonappa; Valkonen, A.; Juvonen, R.; Salo, H.; Kolehmainen, E. Bile acid-derived mono- and diketals—synthesis, structural characterization and self-assembling properties. *Org. Biomol. Chem.* **2010**, *8*, 2784–2794.

(60) Noponen, V.; Nonappa; Lahtinen, M.; Valkonen, A.; Salo, H.; Kolehmainen, E.; Sievänen, E. Bile acid–amino acid ester conjugates: gelation, structural properties, and thermoreversible solid to solid phase transition. *Soft Matter* **2010**, *6*, 3789–3796.

(61) Svobodová, H.; Nonappa; Wimmer, Z.; Kolehmainen, E. Design, Synthesis and Stimuli Responsive Gelation of Novel Stigmasterol-Amino Acid Conjugates. *J. Colloid Interface Sci.* **2011**, *361*, 587–593.

(62) Svobodová, H.; Nonappa; Lahtinen, M.; Wimmer, Z.; Kolehmainen, E. A Steroid-Based Gelator of $A(LS)_2$ Type: Tuning Gel Properties by Metal Coordination. *Soft Matter* **2012**, *8*, 7840–7847.

(63) Lin, Y. C.; Weiss, R. G. A Novel Gelator of Organic Liquids and the Properties of Its Gels[1]. *Macromolecules* **1987**, *20*, 414–417.

(64) Watase, M.; Nakatani, Y.; Itagaki, H. On the Origin of the Formation and Stability of Physical Gels of Di-O-benzylidene-D-sorbitol. *J. Phys. Chem. B* **1999**, *103*, 2366–2373.

(65) Džubák, P.; Hajdúch, M.; Vydra, D.; Hustová, A.; Kvasnica, M.; Biedermann, D.; Marková, L.; Urban, M.; Šarek, J. Pharmacological activities of natural triterpenoids and their therapeutic implications. *Nat. Prod. Rep.* **2006**, *23*, 394–411.

(66) James, J. T.; Dubery, I. A. Pentacyclic Triterpenoids from the Medicinal Herb, Centella asiatica (L.) Urban. *Molecules* **2009**, *14*, 3922–3941.

(67) Kasal, A. Structure and Nomenclature of Steroids. Steroid Analysis, (Eds.: Makin, H. L. J.; Gower, D. B.), Springer Netherlands, Dordrecht, **2010**, pp. 1–25.

(68) Pollier, J.; Goossens, A. Oleanolic Acid. *Phytochem.* **2012**, *77*, 10–15.

(69) Sporn, M. B.; Liby, K. T.; Yore, M. M.; Fu, L.; Lopchuk, J. M.; Gribble, G. W. New Synthetic Triterpenoids: Potent Agents for Prevention and Treatment of Tissue Injury Caused by Inflammatory and Oxidative Stress. *J. Nat. Prod.* **2011**, *74*, 537–545.

(70) Shanmugam, M. K.; Dai, X.; Kumar, A. P.; Tan, B. K. H.; Sethi, G.; Bishayee, A. Oleanolic acid and its synthetic derivatives for the prevention and therapy of cancer: Preclinical and clinical evidence. *Cancer Lett.* **2014**, *346*, 206–216.

(71) Kamble, S. M.; Goyal, S. N.; Patil, C. R. Multifunctional pentacyclic triterpenoids as adjuvants in cancer chemotherapy: a review. *RSC Adv.* **2014**, *4*, 33370–33382.

(72) Liu, J. Pharmacology of oleanolic acid and ursolic acid. *J. Ethnopharmacol.* **1995**, *49*, 57–68.

(73) Wang, X.; Ye, X.-I.; Liu, R.; Chen, H.-L.; Bai, H.; Liang, X.; Zhang, X.-D.; Wang, Z.; Li, W.-I.; Hai, C.-X. Antioxidant activities of oleanolic acid in vitro: Possible role of Nrf2 and MAP kinases. *Chem. Biol. Interact.* **2010**, *184*, 328–337.

(74) Bag, B. G.; Paul, K. Vesicular and Fibrillar Gels by Self-Assembly of Nanosized Oleanolic Acid. *Asian J. Org. Chem.* **2012**, *1*, 150–154.

(75) Bag, B. G.; Majumdar, R. Self-assembly of Renewable Nano-sized Triterpenoids. *Chem. Rec.* **2017**, *17*, 841–873.

(76) Dash, S. K.; Chattopadhyay, S.; Dash, S. S.; Tripathy, S.; Das, B.; Mahapatra, S. K.; Bag, B. G.; Karmakar, P.; Roy, S. Self assembled nano fibers of betulinic acid: A selective inducer for ROS/TNF-alpha pathway mediated leukemic cell death. *Bioorg. Chem.* **2015**, *63*, 85–100.

(77) Viola, J. R.; Leijonmarck, H.; Simonson, O. E.; Oprea, I. I.; Frithiof, R.; Purhonen, P.; Moreno, P. M. D.; Lundin, K. E.; Stromberg, R.; Smith, C. I. E. Fatty acid–spermine conjugates as DNA carriers for nonviral in vivo gene delivery. *Gene Therapy* **2009**, *16*, 1429–1440.

(78) Behr, J. P. Gene Transfer with Synthetic Cationic Amphiphiles: Prospects for Gene Therapy. *Bioconjugate Chem.* **1994**, *5*, 382–389.

(79) Geall, A. J.; Taylor, R. J.; Earll, M. E.; Eaton, M. A. W.; Blagbrough, I. S. Synthesis of Cholesteryl Polyamine Carbamates: pKa Studies and Condensation of Calf Thymus DNA. *Bioconjugate Chem.* **2000**, *11*, 314–326.

(80) Blagbrough, I. S.; Hadithi, D. A.; Geall, A. J. Cheno-, Urso- and Deoxycholic Acid Spermine Conjugates: Relative Binding Af®nities for Calf Thymus DNA. *Tetrahedron* **2000**, *56*, 3439–3447.

(81) Smith, D. K. From fundamental supramolecular chemistry to self-assembled nanomaterials and medicines and back again – how Sam inspired SAMul. *Chem. Commun.* **2018**, *54*, 4743–4760.

(82) Merritt, M.; Lanier, M.; Deng, G.; Regen, S. L. Sterol-Polyamine Conjugates as Synthetic Ionophores. *J. Am. Chem. Soc.* **1998**, *120*, 8494–8501.

(83) Janout, V.; Regen, S. L. Bioconjugate-Based Molecular Umbrellas. *Bioconjug Chem.* **2009**, *20*, 183–192.

(84) Lu, Y. M.; Deng, L. Q.; Huang, X.; Chen, J. X.; Wang, B**.;** Zhou, Z. Z.; Hua, G. S.; Chen, W.H. Synthesis and anionophoric activities of dimeric polyamine–sterol conjugates: the impact of rigid vs. flexible linkers. *Org. Biomol. Chem.* **2013**, *11*, 8221–8227.

(85) Sadownik, A.; Deng, G.; Janout, V.; Regen, S. L. Rapid Construction of a Squalamine Mimic. *J. Am. Chem. Soc.* **1995**, *117*, 6138–6139.

(86) Kim, H. S.; Choi, B. S.; Kwon, K. C.; Lee, S. O.; Kwak, H. J.; Leeb, C. H. Synthesis and Antimicrobial Activity of Squalamine Analogue. *Bioorg. Med. Chem.* **2000**, *8*, 2059–2065.

(87) Chen, W. H.; Shao, X. B.; Moellering, R.; Wennersten, C.; Regen, S. L. A Bioconjugate Approach toward Squalamine Mimics: Insight into the Mechanism of Biological Action. *Bioconjugate Chem.* **2006**, *17*, 1582–1591.

(88) Dewangan, R. P.; Jain, A.; Tanwar, S.; Yar, M. S.; Pasha, S. Self assembly and hydrogelation of spermine functionalized aromatic peptidomimetics against planktonic and sessile methicillin resistant S. aureus. *RSC Adv.* **2016**, *6*, 112656–112666.

(89) Gabrielson, N. P.; Cheng, J. Multiplexed Supramolecular Self-Assembly For Non-Viral Gene Delivery. *Biomaterials* **2010**, *31*, 9117–9127.

(90) Bildziukevich, U.; Vida, N.; Rárová, L.; Kolář, M.; Šaman, D.; Havlíček, L.; Drašar, P.; Wimmer, Z. Polyamine Derivatives of Betulinic Acid and β-Sitosterol: A Comparative Investigation. *Steroids* **2015**, *100*, 27–35.

(91) Bildziukevich, U.; Kaletová, E.; Šaman, D.; Sievänen, E.; Kolehmainen, E. T.; Šlouf, M.; Wimmer, Z. Spectral and Microscopic Study of Self-assembly of Novel Cationic Spermine Amides of Betulinic Acid. *Steroids* **2017**, *117*, 90–96.

(92) Bildziukevich, U.; Malík, M.; Özdemir, Z.; Rárová, L.; Janovská, L.; Šlouf, M.; Šaman, D.; Šarek, J.; Nonappa; Wimmer, Z. Spermine Amides of Selected Triterpenoid Acids: Dynamic Supramolecular Systems Formation Influences Cytotoxicity of the Drugs. *J. Mater. Chem. B* **2020**, *8*, 484–491.

(93) Goddard-Borger, E.D.; R. V. Stick, R. V. An Efficient, Inexpensive, and Shelf-Stable Diazotransfer Reagent: Imidazole-1-sulfonyl Azide Hydrochloride. *Org. Lett.* **2007**, *9*, 3797–3800.

(94) Fischer, N.; Goddard-Borger, E. D.; Greiner, R.; Klapötke, T. M.; Skelton, B. W.; Stierstorfer, J. Sensitivities of Some Imidazole-1-sulfonyl Azide Salts. *J. Org. Chem.* **2012**, *77*, 1760–1764.

(95) Huisgen, R. 1,3-Dipolar Cycloadditions Past and Future. *Angew. Chem. Int. Ed. Engl.* **1963**, *2*, 633–645.

(96) Li, H.; Aneja, R.; Chaiken, I. Click Chemistry in Peptide-Based Drug Design. *Molecules* **2013**, *18*, 9797–9817.

(97) Tron, G. C.; Pirali, T.; Billington, R. A.; Canonico, P. L.; Sorba, G.; Genazzani, A. A. Click Chemistry Reactions in MedicinalChemistry: Applications of the 1,3-dipolar Cycloaddition Between Azides and Alkynes. *Med. Res. Rev.* **2008**, *28*, 278–308.

(98) Cheng, K.; Liu, J.; Liu, X.; Li, H.; Sun, H.; Xie, J. Synthesis of glucoconjugates of oleanolic acid as inhibitors of glycogen phosphorylase. *Carbohydrate Res.* **2009**, *344*, 841–850.

(99) Özdemir, Z.; Bildziukevich, U.; Šaman, D.; Havlíček, L.; Rárová, L.; Navrátilová, L.; Wimmer, Z. Amphiphilic Derivatives of (3β,17β)-3-Hydroxyandrost-5-ene-17-carboxylic Acid. *Steroids* **2017**, *128*, 58–67.

(100) Bertula, K.; Martikainen, L.; Munne, P.; Hietala, S.; Klefström, J.; Ikkala, O.; Nonappa Strain-Stiffening of Agarose Gels. *ACS Macro Lett.* **2019**, *8*, 6670–6675.

(101) Sollich, P. in Molecular Gels, Materials with Self-Assembled Fibrillar Networks, (Eds.: Weiss, R. G.; Terech, P.), Springer, Dordrecht, Netherlands, **2006**, pp. 161–192.

SYNOPSIS

For the Table of Contents Only:

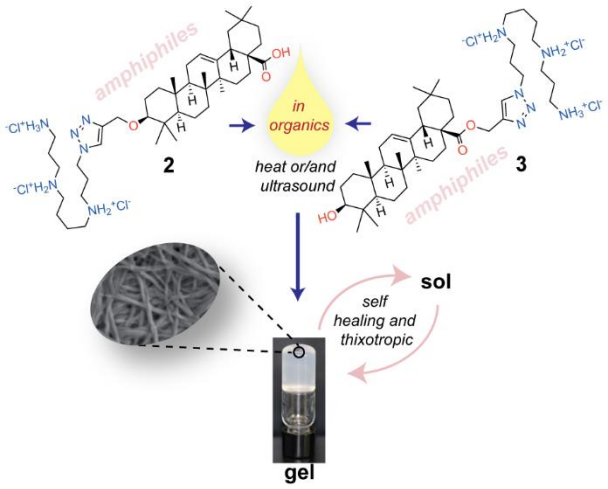

Self-assembly of strategically designed oleanolic acid-triazole-spermine conjugates are reported, showing that these amphiphiles undergo spontaneous gelation in organic solvents displaying a mixed self-healing and thixotropic properties.